

# **Thesis Summary**

**Faculty of Physics, University of Bucharest**

**Phase transition from hadronic gas to plasma of quarks and gluons and possible critical points. Application for the CBM experiment**

**Author: Nicolae George Țuțuraș**

**Scientific coordinator: Prof. univ. dr. Alexandru Jipa**

Defended on May 25<sup>th</sup>, 2023

In this thesis, I present some results related to nuclear matter phase transitions created by relativistic nuclear collisions. The strongly interacting matter at high baryonic densities is still full of enigmas. Also, the complexity of the final state of the collision between two heavy ions for high energies requires the extraction of significant information, which implies systematic experimental measurements, as complete as possible, which include the excitation functions, the dependencies on the system's dimensions and the multi-differential distributions in the phase space of the identified particles. An analogy can be made between the processes that characterize the evolution of the early Universe and those that can be produced in the laboratory by the collision of nuclei at high energies.

Based on different cosmological scenarios, a specific phase of highly excited and dense nuclear matter, called quark-gluon plasma, would have been formed around  $10^{-6}$  s after the primordial explosion (“Big Bang”). This primordial “soup” has a very short lifetime, being followed by the process of hadron formation. To explore these energy densities from the early moments of the Universe, heavy relativistic ion collisions are studied in the laboratory, due to the fact that in the overlap region of the two colliding nuclei, another region of very hot and extremely compressed nuclear matter is formed, called a “fireball”. The characteristics of this region mimic the properties hypothesized for the matter that filled the early Universe. The theoretical interest in the study of relativistic nuclear collisions has its origin, in part, in the belief that we will be able to explore the quantum vacuum structure of strong interactions and, in particular, the phenomenon of quark confinement. General discussions about the value of the macroscopic Hubble constant, the formation of quark-gluon plasma, and its evolution similar to the general evolution of the Universe according to a Hubble-like law developed in our physics group, as well as some characteristics due to the quantum vacuum are treated in the first chapter of this thesis.

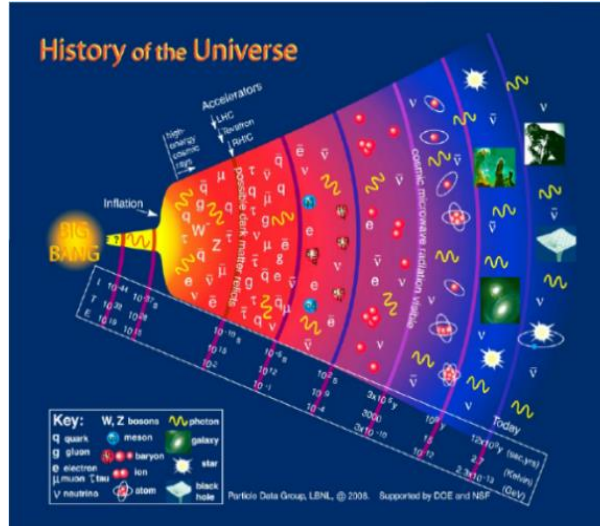


Fig 1. The origin and evolution of the universe [1]

The second chapter of the thesis comprises a presentation of the CBM (Compressed Baryonic Matter) experiment. The research program on dense nuclear and subnuclear matter (Quantum Chromodynamics (QCD) matter) at FAIR (Facility for Antiproton and Ion Research) will be conducted by the CBM and HADES experiments. The scientific program of the CBM experiment is primarily focused on investigating probes originating from the early stages of collisions, for which nuclear matter is highly excited. In this chapter, I present several properties of strongly interacting matter, the production mechanisms of different particles in highly excited and dense matter, as well as the propagation in nuclear matter, considering specific threshold energies. Additionally, characteristics of the detectors used in the CBM experiment are presented. A highly diverse structure of events is expected in the QCD phase diagram, closely related to the baryonic chemical potential, the first-order phase transition between hadronic and partonic matter, the identification of the critical point.

Phase transitions, especially first-order transitions that can lead the hadronic matter to the quark-gluon plasma state, as well as other phase transitions - most of them happening in the early Universe - are discussed in Chapter III. Signals of first-order phase transitions are explored through lattice QCD calculations and benchmark theoretical computations, but also through experimental results.

In Chapter IV of the thesis, results obtained from simulated data for various physical quantities of interest in understanding the dynamics of relativistic nuclear collisions are presented.

The results presented in this thesis are in good agreement with the results from other papers based on experimental data (BES-STAR, KaOS, NA 49). Thus, I present results based on transverse momentum distributions: these calculations allow the determination of apparent temperatures. The obtained values are in good agreement with the types of phase transitions considered. The flow of nuclear matter and the cumulative number can be influenced by fluctuations, which can be an extremely useful analysis tool in the search for the critical point. Therefore, I present computations for the cumulative number associated with the number of positive and negative pions at two centralities, for energies available at FAIR-GSI Darmstadt. Higher moments of multiplicity distributions constitute one of the most sensitive probes in searching for the critical point; results for asymmetry parameters (skewness) and maxima formation parameters (kurtosis) will also be presented, as well as estimates of the “microscopic Hubble constant”.

The excitation function and the particle-antiparticle ratio can be utilized for the study of exotic states and phase transitions in nuclear matter formed in nuclear collisions, as well as for determining “freeze-out” parameters. They can provide clues about hadronization mechanisms. Additionally, these parameters can be used to identify the type of equilibrium state in newly formed matter in relativistic nuclear collisions. The analyses in this thesis were based on simulated data using widely used codes in the field, namely, the UrQMD code and the AMPT code (in the UrQMD 3.3 and AMPT 2.26t7 versions, respectively).

The most important conclusions of the thesis are presented in Chapter V. For the study of particle-antiparticle ratios, the author considered Au-Au collisions at energies available at FAIR-GSI. The energy range considered is between 6 A GeV and 28 A GeV. I examined the evolution of antikaon/kaon and antiproton/proton ratios, as well as kaon/proton or proton/pion ratios in the respective collisions, at various centralities and different rapidity intervals. In the analyses of Au-Au collision simulations at the mentioned energies, I found plateau-like shapes and sudden increases followed by short plateaus for certain values of the particle-antiparticle ratio. This contrasts with general trends that show an increase in the ratio with the increase in collision energy. The plateau-like shapes suggest phase transitions in the highly excited nuclear matter obtained in relativistic nuclear collisions.

I enumerate in the first part of the first chapter of my thesis some aspects for concepts related to the nuclear physics. After 1950, the concept of nuclear matter was introduced. In its normal state, it is composed of nucleons and virtual pions. The discovery of heavy ions with energies per nucleon greater than the rest energy of a nucleon in 1948 paved the way for the observation of nuclear matter in various phases and potential transitions between these phases. Over the years, in order to describe them, different models have been proposed, and new concepts related to the structure of particles - at one point deemed elementary - and to distinct types of interactions were introduced.

The transition from cosmic radiation to accelerator systems for the purpose of creating collisions of relativistic heavy ions has significantly enhanced the ability to characterize nuclear matter formed in the overlap region of colliding heavy ions at relativistic energies. This approach permits a better and deeper understanding of aspects that are challenging to elucidate through other means, aiming for a more accurate phase diagram description of nuclear matter. This diagram would encompass not only normal nuclear matter, but also nuclear matter under different conditions, including densities below normal density and temperatures below the binding energy per nucleon, as well as matter at densities exceeding normal nuclear density and temperatures well above the binding energy per nucleon [1].

Such a phase diagram can contain information from the appearance moment of our Universe to the present stage and beyond. The fundamental concepts are related to Nuclear Physics, Particle Physics, and Cosmology. Therefore, Relativistic Nuclear Physics (Physics of Relativistic Heavy Ions) is considered as a bridge connecting all these domains. It can provide a coherent and adequate perspective on the early Universe and its evolution over billions of years. To understand the phenomena and processes involved, specific concepts are necessary, including those already present in the standard model, with its various components and developments.

One of the most spectacular periods of the early Universe is the one in which quarks and gluons appeared (see Fig 1). According to the specific properties described by Quantum Chromodynamics (QCD), they must've quickly clustered into strongly interacting particles (hadrons). This rapid process (between 100 s and 200 s) is called hadronization. The subsequent stages of nucleosynthesis and the formation of celestial bodies led to the emergence of the world in which we currently live in (see Fig 2 ).

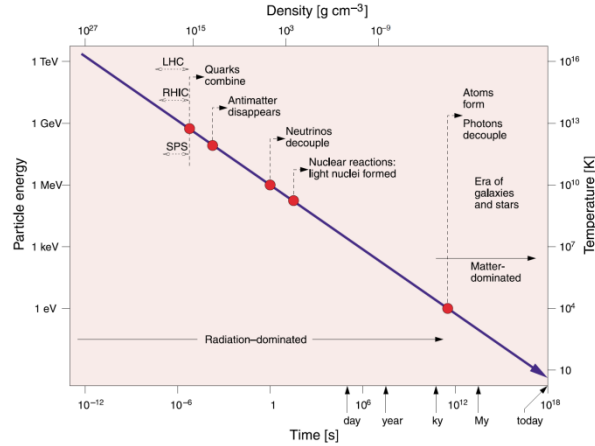


Fig 2. Evolution stages of the Universe and the specific particles produced [2]

The description of the early Universe, in which the QGP state is considered to have existed, as well as the specific processes of hadron and nuclei formation (hadronization and nucleosynthesis, respectively), pose scientific challenges with many unknowns. The research in Relativistic Nuclear Physics can play a crucial role in describing and understanding these phenomena. Additionally, the complex issues related to the restoration of chiral symmetry while still maintaining a confined phase remain subjects of theoretical debate and experimental confirmation. High-precision measurements of multiplicity for hadron species at SIS-100 can be decisive in elucidating the thermal properties of the region participating in chemical “freeze-out” and, consequently, in elucidating the appearance of a possible phase transition at high net baryon densities.

The theoretical interest in the study of relativistic and ultra-relativistic heavy-ion collisions originates from the hypothesis that we can explore the vacuum structure of strong interactions, particularly the phenomenon of quark confinement. Quark confinement couldn't be explained as a direct result of the interactions between quarks, generated by color charge and the exchange of gluons. In the quark-gluon plasma, quasi-free propagation of quarks and gluons is possible. The description of high-energy hadronic interactions, with transitions to deconfined matter, is highly diverse, with various physical implications, justifying the study of interactions within QCD. This description can also be used for understanding characteristics of matter which existed in the early Universe [3].

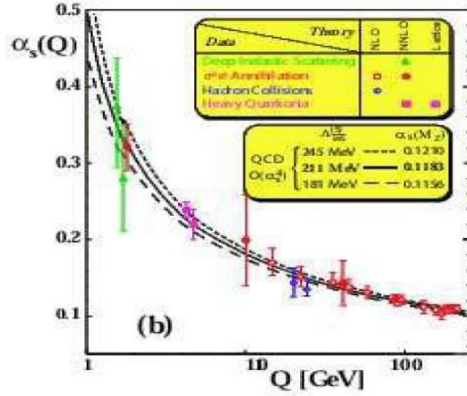


Fig 3. Summary of measurements of  $\alpha_s(Q^2)$  [4]

Due to this fundamental theory, we can describe hadrons as resembling quark bags, i.e., bound states assembled from quarks. Quarks can move freely when they are close - at a distance of about 1 Fm - but are strongly bound when the distance between them increases. This property is called asymptotic freedom (see Fig 3), to which we must add the confinement of color, such that the overall color charge is zero. These properties are included in the model called the Quark Bag Model (MIT), extensively used in calculations. In the first chapter, I presented a series of important quantities and characteristics of processes corresponding to QCD matter, as well as some basic aspects of the confinement-deconfinement phenomenon.

I discuss next the following issues: the effective coupling constant, which describes the probability of an interaction between a quark and a gluon, the variable  $\Lambda_{\text{QCD}}$  which represents the scale of strong interactions and distinguishes between the world of confined hadrons ( $Q^2 \sim \Lambda_{\text{QCD}}^2$ ) and that of free quarks and gluons ( $Q^2 \gg \Lambda_{\text{QCD}}^2$ ). A quark carries a color charge, and an anti-quark carries an anti-color charge, and each gluon has a charge that is a combination of a color charge and an anti-color charge. Since individual quarks have not been observed in nature, it has been postulated that only color singlets (“white” states) are observable in nature. If the distance between two quarks increases, gluon-gluon interactions cause the concentration of color field lines into color tubes, called strings. For large distances, the second term in  $V(r) = \sigma r - \frac{4\alpha_s^2}{3r}$ , where  $\alpha(Q^2) = \frac{12\pi}{(33-2n_f)\ln(Q^2/\Lambda_{\text{QCD}}^2)}$ , is predominant, and the potential increases linearly with the distance between quarks. When the distance becomes sufficiently large, there is enough potential energy to create a new pair. The production of quark-antiquark pairs by breaking the strings is done by strictly respecting the possible color combinations; each system that is produced must maintain

color neutrality. Less energy is required to create two new quarks than to move two quarks far apart. Thus, we obtain two quark pairs instead of one [1,5].

The scenarios for the evolution of the Universe after the “Primordial Explosion“ are developed and verified through the study of collisions of heavy ions at ultra-relativistic and relativistic energies. The correct and comprehensive characterization of the quark-gluon plasma can open a window into the early Universe and, at the same time, can play a crucial role in estimating a quantity called the “microscopic Hubble constant”. Estimating the “microscopic Hubble constant” can assist the physics community in establishing specific connections with the cosmological theories [6]. In the early universe, during the phase transition from the quark-gluon plasma to hadrons, the timescale of expansion was much larger than the timescale for strong interactions,  $\sim 10^{-23}$ s. However, the connection between the Hubble constant corresponding to the evolution of the Universe and the one corresponding to the evolution of the “fireball” in relativistic and ultra-relativistic nuclear collisions can be made by replacing the characteristic constants of Cosmology with those characteristics of the strong interactions of highly excited nuclear matter. In the fourth chapter of my thesis, I will present several evaluations of the decoupling time corresponding to chemical and thermal “freeze-out”, but also estimates of the Hubble constant for these moments in the evolution of the “fireball” as a function of energy. In the final part of the first chapter, I discuss characteristics of the QGP (equation of state) and kinetic signals for its identification. For example, photons and lepton pairs are particles that interact electromagnetically and weakly, being produced in large quantities in the quark-gluon plasma, as mentioned previously. They can be detected without significant influence from strong interactions within the participating region. Direct photons and dileptons created in a relativistic nuclear collision have a large mean free path since they do not strongly interact, which allows them to exit the “fireball” before they interact. Therefore, they can provide information about the hot and very dense state from the early stage of the collision, a phase in which the quark-gluon plasma is believed to have been formed.

In the second chapter, I present the research program on dense nuclear and subnuclear matter at FAIR, which will be conducted by the CBM and HADES experiments. The HADES detector system, with a wide polar angle acceptance ranging from 18 to 85 degrees, has been designed for measurements with proton and heavy-ion beams at moderate particle multiplicities, for example, in Ni-Ni or Ag-Ag collisions at SIS 100 energies [7,8]. Electron pairs and hadrons originating from the decays of various particles, including multi-strange hyperons, are reconstructed with the HADES detector system. It will be possible to conduct experiments over a wide energy range, from 2 A GeV to 45 A GeV, and for different combinations of incident and target nuclei, using the same detector system.

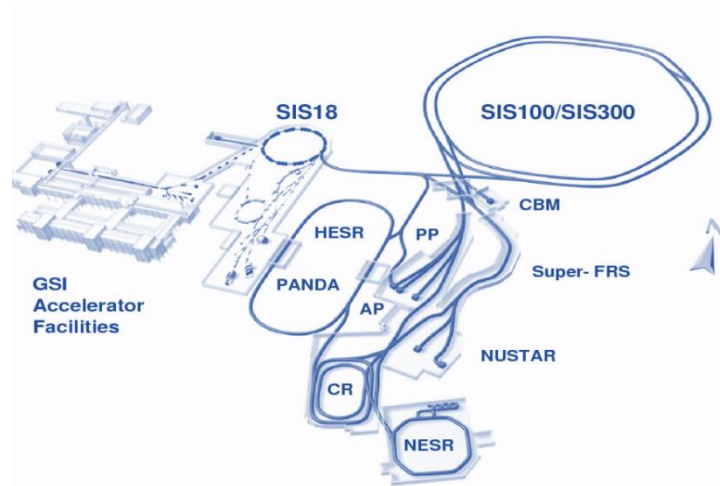


Fig 4. GSI Accelerator Facilities, Darmstadt, Germany [8]

The scientific program of the CBM experiment (Compressed Baryonic Matter) is focused on investigating signals originating from the early stages of collisions for which matter is very dense and highly excited. The CBM experiment is a fixed-target experiment constructed to operate at very high interaction rates, up to 10 MHz, for selected observables (e.g.  $J/\Psi$  decay, at 1-5 MHz, for multi-strange hyperons and dileptons, at 100 kHz). In the energy range of SIS 100, the production and investigation of strongly interacting matter at densities presumed to exist in the cores of neutron stars are expected. The CBM experiment is capable of identifying hyperons in central Au+Au collisions with very high sensitivity, from the decays of strange dibaryons of the following types:  $H \rightarrow \Lambda p - \pi$ ,  $(\Xi^0 \Lambda) b \rightarrow \Lambda \Lambda$  [8,9].



High-precision measurements of the excitation functions of multi-strange hyperons produced in Au+Au collisions at energies available at SIS 100 and SIS 300 will be possible after 2028. These experiments will create conditions for discovering new degrees of freedom of nuclear matter formed in the participating region (“fireball”). Mechanisms for the production of charm particles and their propagation in nuclear matter at threshold energies are also discussed. Model calculations have been performed to estimate the production of “charmonium” in p+A collisions at FAIR energies [10]. At SIS-100, measurements of charm particles can be carried out in reactions induced by protons, using beam energies up to 29 A GeV. Measurements for “open charm” (particles with a single charm quark) are linked to the production of “charmonium” at threshold energies. The production cross-section of “charmonium” can be determined by separately measuring the production of D mesons ( $D^+$ ,  $D^-$ ,  $D^0$ , and  $\text{anti}D^0$ ).

The maximum energy at SIS 100 for Au-Au collisions will be around 10-12 A GeV. The production threshold for “open charm” particles in p+p collisions is approximately 12 GeV. In Au+Au collisions, at the same energy per nucleon, the available energy is about 200 times higher, which can increase the possibility of producing charm particles. This has not been clearly demonstrated experimentally yet. There is a dependence of the production cross-section on the sizes of the probes. Current best estimates suggest that “open charm” particles may not be measurable in Au+Au collisions at 11 A GeV in the CBM experiment. This may only be possible for Ni+Ni collisions at 15 A GeV or p+C collisions at 30 GeV (private communications of the author, see refs.) [11]. The CBM detector system was built as a multi-purpose device and will be able to measure hadrons, electrons, and muons originating from elementary nucleon or heavy ion collisions across the entire spectrum of beam energies provided by FAIR. Measurements of hypernuclei, leptons pairs, or charm particles require detection systems with high rates. The CBM experimental setup is specifically designed to meet these requirements. At the end of the chapter, I present methods for measuring hyperons, hypernuclei, strange dibaryons, dielectrons, and D mesons.

In Chapter III, I provided an overview on the phase transitions: first-order phase transition, mixed phase, electroweak and QCD phase transitions, which are predicted by theoretical calculations, experimental results and lattice QCD calculations. In particular, I discussed possible phase transitions of an ideal gas. Thus, I considered the properties of quark-gluon plasma, initially modeled through an ideal gas of quarks and gluons in chemical equilibrium, which may include the effect of a confining vacuum structure. I also delved into the description of first-order phase transitions signals through lattice QCD calculations, benchmark theoretical calculations, and experimental results.

The issue of the phase transition order, whether it is a first-order phase transition or not, is still under investigation. This is because the order of the phase transition depends on the masses of the quarks used in calculations. As the system cools, it undergoes hadronization, and ultimately experiences chemical “freeze-out” at a temperature around 160 MeV [12]. This temperature coincides with the transition temperature predicted by lattice QCD calculations [13], which suggest a crossover from hadronic to partonic matter [14,15]. On the other hand, some model calculations predict significant phenomena in the QCD phase diagram at substantial baryonic potentials, such as the existence of a critical point.

The experimental results obtained by the NA49 Collaboration at SPS-CERN suggest that we exceed the "boundary" of phases for Pb+Pb collisions in the energy range of the incident beam between 30 A GeV and 60 A GeV. This transition is referred to as the beginning of deconfinement. According to some authors, the most natural description of the results is one that considers both chiral symmetry restoration and deconfinement in the very high energy density phase. There are authors who consider that many relativistic nuclear collision simulations indicate, at energies lower than SPS, just a phase transition of “rapid transit of the phase separation surface” (“rapid cross-over”).

There are many uncertainties in current theoretical models, and the lack of reliable experimental data still does not allow for an unequivocal determination of whether the phase transition is a first-order transition (with a mixed phase) or a “rapid transit of the phase separation surface” (“rapid cross-over”), without a mixed phase. Only the discovery of the critical point can shed light on the boundary properties of the phase transition [11]. Other authors consider possible and even auspicious the existence of phase transitions related to the partial restoration of chiral

symmetry. In this way, a confined phase is still maintained. This remains a subject of theoretical debate and experimental confirmation. One of the remarkable results that can be obtained within the CBM collaboration at FAIR-GSI is related to the behavior of the temperature of the particle-emitting source (hot and dense participant region (“fireball”)) under different conditions, depending on the available energy in the center-of-mass system ( cms). The simulations indicate a flattening of the temperature dependence as a function of the available energy in the center of mass, and that saturation-like behavior persists over an extended range of energies [17]. My results related to antiparticle to particle ratios, for 6-14 A GeV, 18-21 A GeV energy intervals for Au+Au collisions, display saturation/plateau behavior, which can be interpreted as a transition, even a transition of the first order. The increase of these quantities with increasing collisions energy of heavy ions is confirmed by the experiment and this behavior is also seen in my results. In contrast to this general trend, we notice some local trend of equality and quasi-drops of the  $\bar{p}/p$  ratio [11,16,17].

In chapter IV I present results obtained with UrQMD (Ultra-relativistic Quantum Molecular Dynamics) code [18]. This is a simulation code for heavy-ion collisions and has become over time a trusted tool for interpreting many processes that occur in this type of phenomenology. It includes the possibility of estimating particle production, collective flow, and correlation functions. Hadronic states can be produced as a result of string breaking, s-channel collisions, or resonance decays. It is a development of a code initiated by German physicists and was initially called Relativistic Quantum Molecular Dynamics. The code is based on a microscopic model that considers the covariant propagation of hadrons on classical trajectories in combination with stochastic binary scatterings, string formation with color confinement, and resonance decays. In the doctoral thesis, 100000 events were considered for Au-Au collisions at each of the energies of 6, 8, 10, 11.5, 11.12, 13, 16, 20, 25, and 28 A GeV. In these simulations, a time of reaching the “freeze-out” of 200 Fm/c was considered, which could involve up to 1800 binary collisions within the participant region. Values between 0 Fm and 13 Fm were chosen for the impact (collision) parameter. Particles that normally decay ( $\pi$ , K,  $\Delta$ ,  $\Lambda$ ,  $\eta$ , etc.) are not considered stable, and the equation of state is defined by the CASCADE module in the code, referring to the partonic transport mode.

AMPT (A Multi-Phase Transport) is based on a transport model [19]. This is another transport code that takes into account the phenomenology of relativistic heavy-ion collisions. It is a multi-module code. Therefore, it can be considered to have one module for event generation (HIJING – Heavy Ion Jet Interactions Generator), and another for partonic scatterings (ZPC - Zhang's Parton Cascade). Additionally, hadronic scatterings are treated in the end with another module called ART (A Relativistic Transport).

For the simulations conducted for the doctoral thesis, I primarily used the string fragmentation model and a baryon stopping mechanism known as a "popcorn" type mechanism. In the case of simulations with the AMPT code, the same number of events and the same energy values as for the UrQMD code were considered. In this case, due to the code's structure, time intervals of 0.2 Fm/c and 150 steps for the hadronic cascade were considered before the end. The impact parameter was chosen, for the same reasons as in the UrQMD code, between 0 and 13 Fm. Two models are available for the hadronization process: the string fragmentation model, in the transport model underlying the AMPT simulation code, as well as the "melting of strings" model. For the computational simulations, I predominantly employed the string fragmentation model and a baryon stopping mechanism also known as a "popcorn" type mechanism.

The studies conducted were carried out using the YaPT system (Yet another High Energy Physics Tool) [20], within the "Extreme Nuclear Matter" Research Center of the Faculty of Physics, University of Bucharest. YaPT is a platform for generating and analyzing events specific to High Energy Physics, integrating the UrQMD and AMPT generation codes.

The YaPT system consists of two distinct, separate modules: one for Monte Carlo generation, and the other for ROOT analysis. The default ROOT analysis macros are applied to Monte Carlo generated files through the Simulation Service, which is a collection of PHP scripts that execute the generation and analysis processes.

I have performed over 250 simulations for Au-Au collisions (with 100000 events for each collision type and even 1000000, especially in the regions of interest, to thoroughly verify/clarify the behavior/the results of the initial simulations) for the analysis conducted in this thesis, using predictions based on the results obtained with the UrQMD and AMPT simulation codes. The estimations of hadrons ratios - as a function of the transverse and total momentum, as well as

rapidity - and their multiplicities are of great importance for the phase transitions in nuclear matter, including the start condition for quark-gluon plasma formation. Some details about global physical quantities with the YaPT system containing dynamic information are included in Figure 5-8.

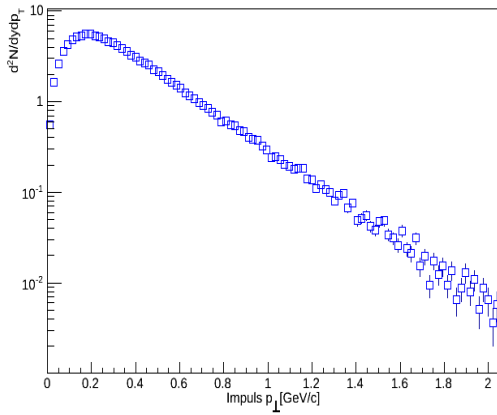


Fig 5. Transverse momentum distribution for  $-0.5 < y < 0.5$ , for negative pions, 0-20% centrality, at 10 A GeV, Au-Au, UrQMD

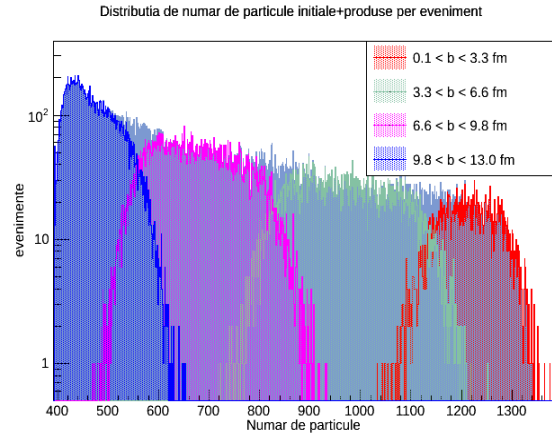


Fig 6. Distribution of initial number of particles produced per event, simulated in YaPT system, Au-Au, UrQMD

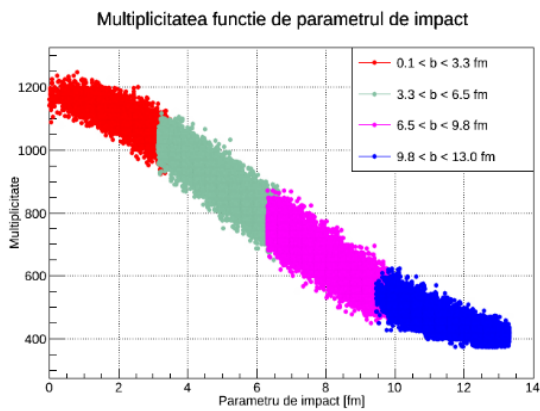


Fig 7. Multiplicity function depending on the impact parameter, Au Au, UrQMD - 12.5 A GeV

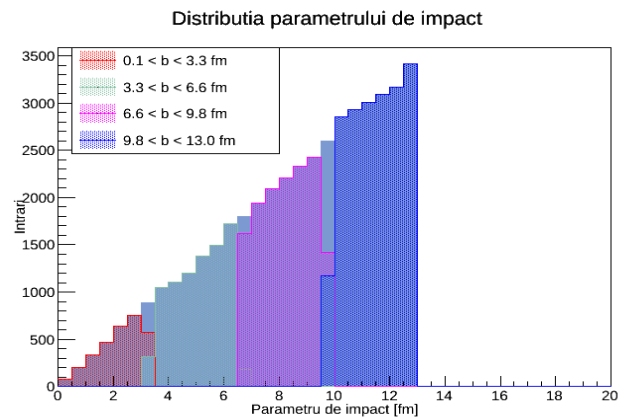


Fig 8. Impact parameter distribution, Au-Au, UrQMD

Calculations based on lattice QCD suggest that higher-order moments of these distributions are sensitive to the phase structure of hot and dense nuclear matter created in relativistic nuclear collisions. Cumulants of parameters associated with processes involving such fluctuations can be sensitive to the proximity of the critical point. In Figure 9, recent results from the STAR collaboration [21] are presented. The value (variance) of the net proton multiplicity distribution is shown as a function of collision energy for Au+Au collisions at the maximum energy available at RHIC-BNL. In models of relativistic nuclear collision dynamics, in the absence of a critical point, this physical quantity is constant, regardless of the collision energy. The presence of a critical point is expected to lead to a non-monotonic behavior of the observable. For the most central collisions, the data obtained at STAR-BES show a deviation from the unit, as expected for critical behavior. [21]

The higher moments of multiplicity distributions are one of the most sensitive probes for searching the critical point, as they are assumed to reflect large fluctuations associated with the hadron-quark phase transition. The net number of protons—defined as the number of protons minus the number of antiprotons — or the fluctuations in the event-by-event analysis of the net number of kaons, both experimentally determinable quantities, can provide information about the baryonic number and charge fluctuations. Thus, higher moments of the multiplicity distributions of these quantities can be used to search for the QCD critical point in relativistic heavy-ion collisions.

For example, for the third-order moment used in the definition of the asymmetry parameter (“skewness”), a change in sign is expected when the system's evolution trajectory on the phase diagram crosses the boundary (separation region) between phases [21]. A similar result is anticipated for the maximum formation parameter (“kurtosis”). In Figure 10, the behavior of the maximum formation (“kurtosis”) parameters can be observed [23].

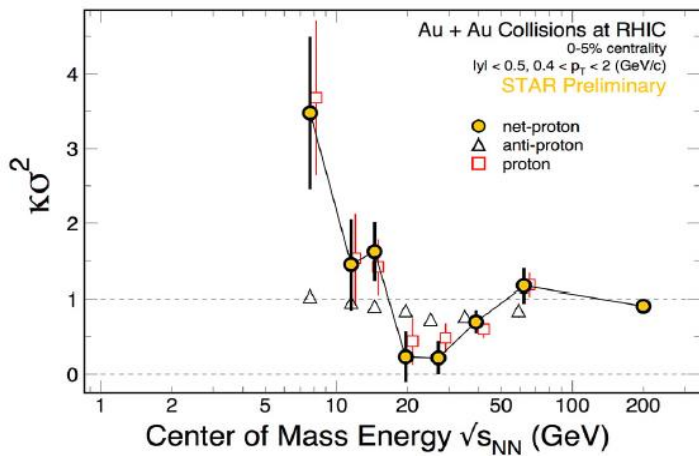


Fig 9. The behavior of  $\kappa\sigma^2$  of the proton multiplicity distribution depending on energy [21]

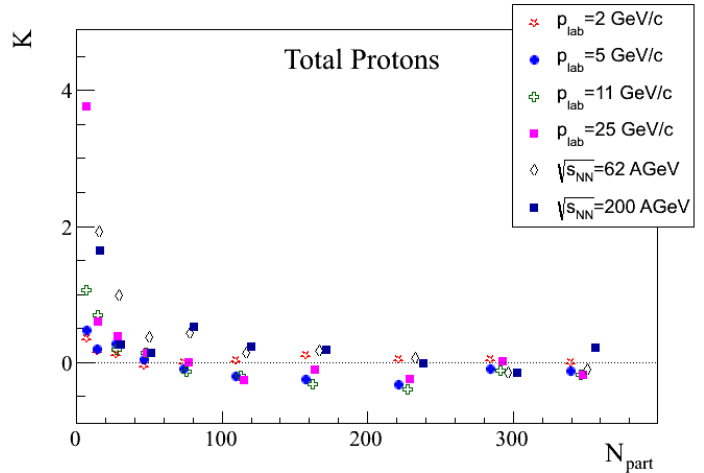


Fig 10. The behavior of kurtosis maximum formation parameter, for Au-Au collisions, at different energies - UrQMD [23]

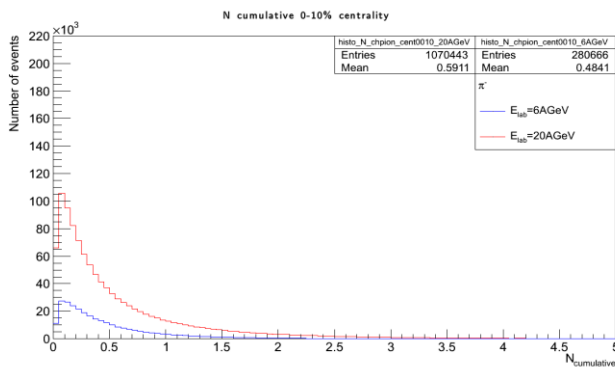


Fig 11. Cumulative number for negative pions, 0-10% centrality, for Au-Au collisions at 6 A GeV and 20 A GeV - UrQMD

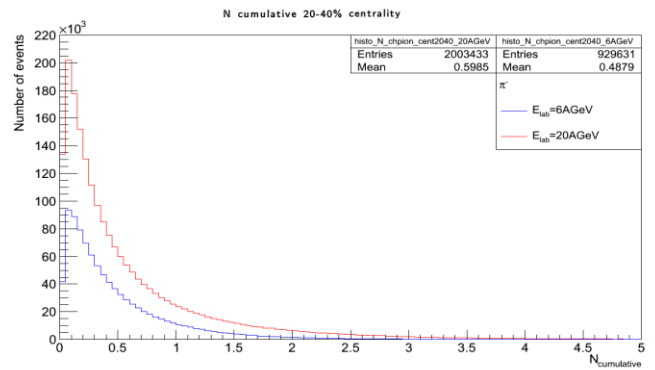


Fig 12. Cumulative number for negative pions, 20-40% centrality, for Au-Au collisions at 6 A GeV and 20 A GeV - UrQMD

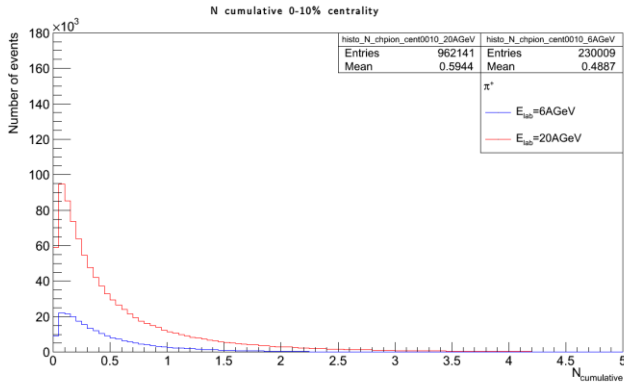


Fig 13. Cumulative number for positive pions, 0-10% centrality, for Au-Au collisions at 6 A GeV and 20 A GeV - UrQMD

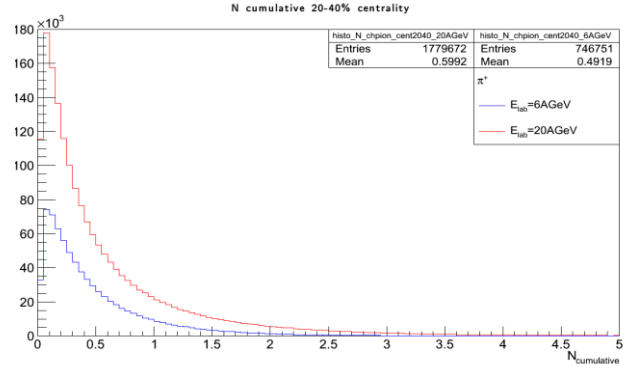


Fig 14. Cumulative number for positive pions, 20-40% centrality, for Au-Au collisions at 6 A GeV and 20 A GeV - UrQMD

Another interesting result from our group, obtained from a global analysis, suggests the absence of nuclear matter jets in the most central nucleus-nucleus collisions at relativistic energies. In such collisions, there is a possibility of achieving a high degree of thermalization. The number of jets increases with the collision parameter's value. The formation of jets can be correlated with the flow of nuclear matter, and with the occurrence of some phase transitions. Considering that the cumulative effect and the jet formation may be related to the partonic structure of nuclear matter, an analysis of such aspects has been conducted for collisions expected to take place at CBM energies.

Estimates for the cumulative numbers (see Figures 11,12,13,14) and the models for the formation of complex parton systems that allow the production of particles with anomalous kinematics compared to nucleon-nucleon collision kinematics, at the same energy, can be important indicators of the formation of phase transitions of nuclear matter at the energies available at SIS-100 (FAIR-GSI).

The connection between the Hubble constant corresponding to the evolution of the Universe and a possible constant associated with the evolution of the “fireball” in relativistic and ultra-relativistic nuclear collisions can be established by replacing the characteristic constants of Cosmology with those of the strong interaction from the “fireball” level. In the present study, taking into account the hydrodynamic evolution of the fireball, we estimate the microscopic Hubble constant and the evolution time using experimental results published by scientific



collaborations from AGS-BNL, SPS-CERN, RHIC-BNL and LHC-CERN.[24]. We estimated a microscopic Hubble constant around  $10^{23} \text{ s}^{-1}$  based on a Stefan- Boltzmann type equation of state [24].

We estimate thus the "microscopic" Hubble-like parameter for relativistic nuclear collisions, similar to the cosmological Hubble constant. The obtained relation is:

$$G_N = \frac{\hbar c}{m_{Pl}^2} \rightarrow N = C \cdot \frac{\alpha_s \hbar c}{m_\pi^2}$$

where C is a proportionality constant,  $\alpha_s$  is the strong coupling constant, and  $m_\pi$  is the rest mass of the pion.

The decoupling time at chemical “freeze-out” time for heavy-ion collisions at different energies was calculated using equation:

$$t = \frac{2}{3} \sqrt{\frac{3}{8\pi N\epsilon}} = \frac{2}{3} \sqrt{\frac{3m_\pi^2}{8C\pi\alpha_s\hbar c \frac{\pi^2 T^4}{10}}}$$

The decoupling time for the case of chemical freeze-out can be extracted from the particle ratios slope using fits with the chemical equilibrium model [24] for the above equation. The results are shown in Table 1. It is observed that the temperature at chemical “freeze-out” increases with the increase in collision energy.

I show in Table 2 the decoupling time at thermal freeze-out, which was obtained using the same formula. Further, by implementing blast-wave fits to transverse momentum distributions for a class of particles, the thermal freeze-out temperatures can be plotted.

$\sqrt{s_{NN}}$ [GeV]	$T_{ch}$ [MeV]	$t_{ch}^{FO}$ [Fm/c]	$H_{ch} \cdot 10^{23}$ [ $\text{s}^{-1}$ ]
1.91	$49 \pm 3$	$23.75 \pm 2.91$	$0.084 \pm 0.010$
2.24	$54 \pm 2$	$19.56 \pm 1.45$	$0.102 \pm 0.007$
2.67	$70 \pm 10$	$11.64 \pm 3.32$	$0.172 \pm 0.049$
4.8	$125 \pm 3$	$3.65 \pm 0.18$	$0.548 \pm 0.026$
6.27	$134 \pm 5$	$3.18 \pm 0.24$	$0.630 \pm 0.047$
7.62	$142 \pm 4$	$2.83 \pm 0.16$	$0.707 \pm 0.040$
8.8	$146 \pm 4$	$2.67 \pm 0.15$	$0.748 \pm 0.041$
12.3	$153 \pm 5$	$2.44 \pm 0.16$	$0.821 \pm 0.054$
17.3	$168 \pm 5$	$2.02 \pm 0.12$	$0.990 \pm 0.059$
62.4	$154.4 \pm 9.9$	$2.39 \pm 0.31$	$0.836 \pm 0.107$
130	$154.2 \pm 9.7$	$2.40 \pm 0.30$	$0.834 \pm 0.105$
200	$159.3 \pm 5.8$	$2.25 \pm 0.16$	$0.890 \pm 0.065$

Table 1. Collision energy, chemical freeze-out temperature, the decoupling time at chemical freeze-out and the microscopic Hubble constant at chemical freeze-out [24]

$\sqrt{s_{NN}}[GeV]$	$T_{ch}[MeV]$	$t_{ch}^{FO}[Fm/c]$	$H_{ch} \cdot 10^{23}[s^{-1}]$
1.98	$26.2 \pm 5.1$	$83.08 \pm 16.17$	$0.024 \pm 0.005$
2.05	$36.7 \pm 7.5$	$42.34 \pm 8.65$	$0.047 \pm 0.009$
2.14	$59.0 \pm 15.5$	$16.38 \pm 4.30$	$0.122 \pm 0.032$
4.8	$127 \pm 10$	$3.54 \pm 0.28$	$0.566 \pm 0.045$
8.8	$134 \pm 5$	$3.18 \pm 0.12$	$0.630 \pm 0.024$
12.3	$127 \pm 7$	$3.54 \pm 0.19$	$0.566 \pm 0.031$
17.3	$125 \pm 5$	$3.65 \pm 0.15$	$0.548 \pm 0.022$
62.4	$98.7 \pm 10.2$	$5.85 \pm 0.60$	$0.342 \pm 0.035$
130	$96.5 \pm 8.0$	$6.12 \pm 0.51$	$0.327 \pm 0.027$
200	$89 \pm 12$	$7.20 \pm 0.97$	$0.278 \pm 0.038$

Table 2. Collision energy, thermal freeze-out temperature, the decoupling time at thermal freeze-out and the microscopic Hubble constant at thermal freeze-out [24]

The "microscopic" Hubble constant at chemical "freeze-out" increases with the increase in energy. The expansion rate of the system is higher. The microscopic Hubble constant is larger for chemical "freeze-out" than the microscopic Hubble constant for thermal "freeze-out", and the system reaches chemical "freeze-out" faster.

$\sqrt{s_{NN}}[GeV]$	$\langle\beta_{tr}\rangle$	$\beta_s$	$R_{ch}[Fm]$
8.8	$0.450 \pm 0.020$	$0.675 \pm 0.020$	$3.844 \pm 0.151$
12.3	$0.470 \pm 0.020$	$0.705 \pm 0.020$	$3.788 \pm 0.190$
17.3	$0.480 \pm 0.020$	$0.720 \pm 0.020$	$3.412 \pm 0.154$
62.4	$0.554 \pm 0.018$	$0.720 \pm 0.011$	$3.416 \pm 0.488$
130	$0.567 \pm 0.020$	$0.765 \pm 0.014$	$4.762 \pm 0.458$
200	$0.592 \pm 0.051$	$0.835 \pm 0.042$	$5.231 \pm 0.849$

Table 3. The energy, the transverse collective flow velocity, the surface collective flow velocity and the system size at chemical freeze-out for different systems produced in heavy ion collisions at various energies [24]

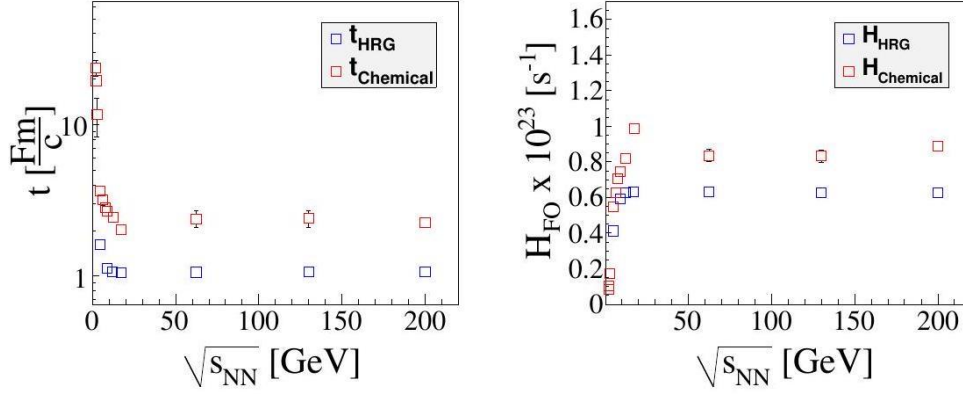


Fig 15. Left: The chemical freeze-out time (red) and Hubble constant at the chemical freeze-out stage for the HRG case with excluded volume corrections as a function of the beam energy (blue). Red points are the calculations made for the ideal pionic gas [24].

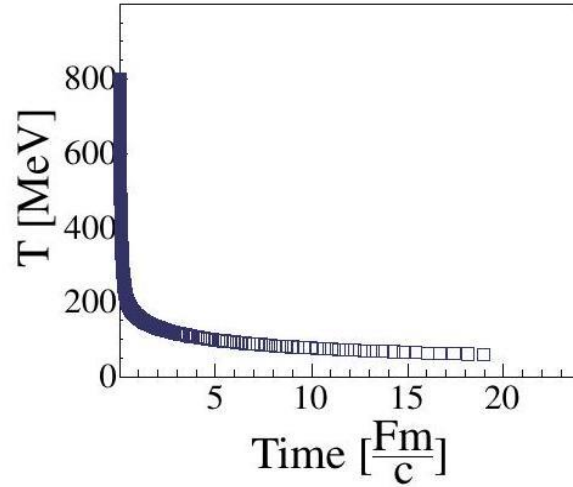


Fig 16. System temperature vs. time considering an EOS based on the lattice approach in the high temperature region, while using the resonance gas equation of state in the low temperature region [24]

Using s95p-v1 parametrization for the EOS [24], we obtained the time evolution for a fireball which is in the early stages in the QGP phase and due to subsequent cooling during the expansion it reaches hadronic phase. It can be seen from Figure 16 that the "fireball" is in the QGP state only for a very short time, less than  $1 \frac{\text{Fm}}{c}$ , after which phase transition to hadronic gas occurs. From the calculations, it can be observed that the "fireball" reaches thermal "freeze-out" in a time interval of the order of  $5\text{-}10 \frac{\text{Fm}}{c}$  [24].

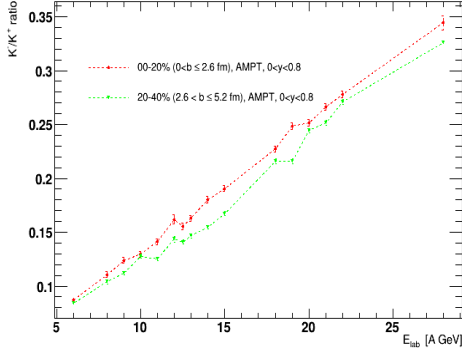


Fig 17.  $\frac{K^-}{K^+}$  ratio distribution for two centralities, rapidity interval  $0 < y < 0.8$  and different collision energies, AMPT[25]

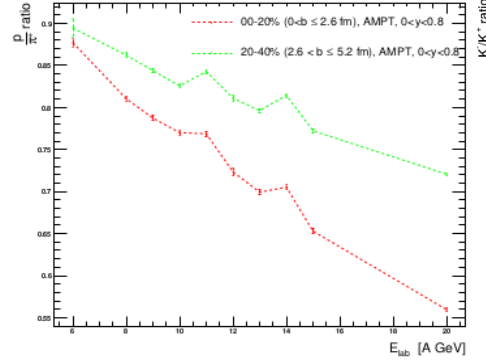


Fig 18.  $\frac{p}{\pi^+}$  ratio distribution for two centralities, rapidity interval  $0 < y < 0.8$  and different collision energies, AMPT [26]

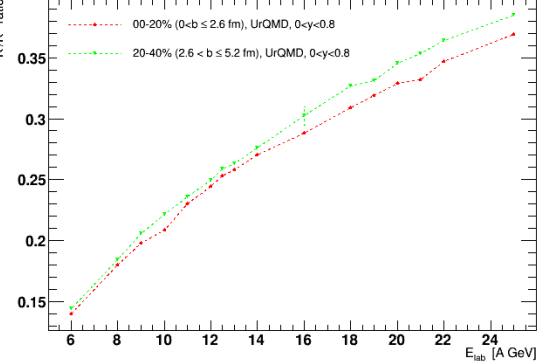


Fig 19.  $\frac{K^-}{K^+}$  ratio distribution for two centralities, rapidity interval  $0 < y < 0.8$  and different collision energies, UrQMD [27]

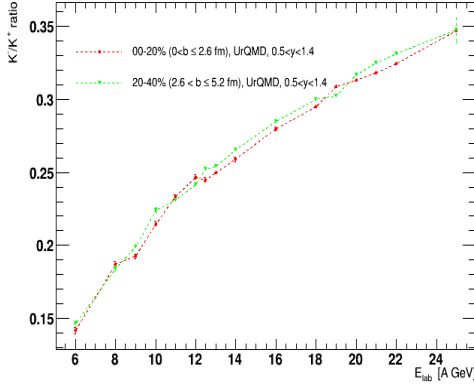


Fig 20.  $\frac{K^-}{K^+}$  ratio distribution for two centralities, rapidity interval  $0.5 < y < 1.4$  and different collision energies, UrQMD [27]

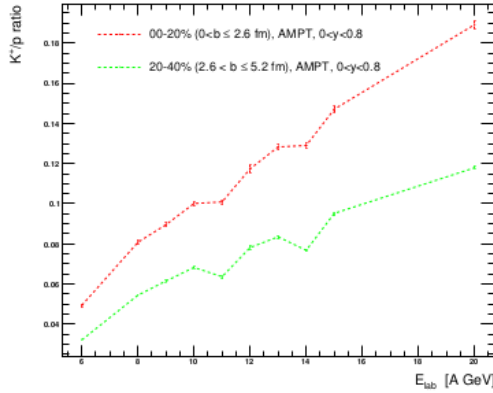


Fig 21.  $\frac{K^+}{p}$  ratio distribution for two centralities, rapidity interval  $0 < y < 0.8$  and different collision energies, AMPT [26]

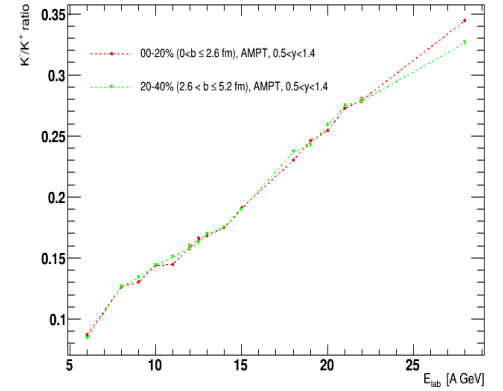


Fig 22.  $\frac{K^-}{K^+}$  ratio distribution for two centralities, rapidity interval  $0.5 < y < 1.4$  and different collision energies, AMPT [25]

The excitation function for various types of particles considered for the evaluation of particle-antiparticle ratios allows the study of exotic states (the existence of density isomers) and of phase transitions in nuclear matter formed in relativistic heavy-ion collisions. Additionally, the values are useful in determining the “freeze-out” parameters and also for eliminating volume fluctuations. For the antikaon/kaon ratio, the predictions of the AMPT code (see Figure 17), in the case of Au+Au collisions at various energies, for the rapidity interval  $0 < y < 0.8$ , show fluctuations within the 10-14 A GeV range. Thus, a quasi-linear increase is observed both below and above the

specified energy range, with short plateaus. Similarly, for the  $K/p$  and  $p/\pi$  ratios (see Figures 21,18), the non-monotonic character is evident (for the specified interval). In experiments conducted at energies which will be available at SIS 100, energy densities up to 7 times the normal density  $\rho_0$  are reached in central Au-Au collisions at energies around 10 A GeV. Discontinuities or a sudden variation in the excitation function of sensitive observables can indicate a phase transition for conditions of strongly compressed nuclear matter.

An important observation is that  $K^-/K^+$  ratios values (see Figures 19, 20, 22) are higher for the 20-40% centrality (compared to 00-20% centrality) - for the UrQMD code. This higher value of the  $K^-/K^+$  ratio for the 20-40% centrality is also observed in the results obtained by other experiments, at energies up to 3 A GeV e.g. the KaoS Experiment. An explanation of the  $K^-/K^+$  ratio increase could be related to a higher production rate of  $K^-$ , which was connected to the effective mass reduction of the negative kaon due to the increased amplitudes in the strangeness exchange channel. More recent data suggest a higher proportion of about 20% for the production of  $K^-$  resulting from the decays of  $\Phi$  ( see references from [27]).

In the intervals 10-14 A GeV, and 18-21 A GeV, respectively, where we can see equal values of the ratios, i.e. a temporization of the excitation function that can influence the antiparticle-particle ratios, the emergence of a mixed phase for a very short time can be suggested. I observed a different behavior of the ratio  $\frac{\bar{p}}{p}$  for 11 and 13 A GeV (for example, UrQMD,  $0 < y < 0.8$ , 00-20% - see Figure 23) with the step of 2 A GeV. For a clarification of the behavior, we used intervals of 1 A GeV for the excitation function and even 0.5 A GeV, to see such phenomenon: quasi-decline (plateau) ratio, which may suggest the switching to a mixed phase, for a fraction of time [25,26,27]. For the interval  $0.5 < y < 1.4$  a  $\frac{\bar{p}}{p}$  peak at 18 A GeV is observed followed by a short plateau (see Figure 24), then a new exponential increase in the antiparticle/particle ratio values [25,27].

The slope of the graph is steep in this case, for the excitation function, which can influence the value of the antiparticle-particle ratio. One may interpret that a maximum is forming, followed by two lower ratio values placed on a short plateau and then an exponential increase in values is seen, which may be in agreement with the prediction of a possibly first order phase transition.

This result can be correlated with some of the theoretical predictions of Gorenstein, Gazdzicki and Bugaev for a start of deconfinement for this energy [28] and also with the results from [17] which show us the excitation function of the fireball temperature, which is extracted

from intermediate dilepton mass distributions - which show a caloric curve that flattens (plateau forms). This plateau corresponds to the conditions in which the first-order transition is presumed in nucleus-nucleus collisions at the available SIS-100 energies [17].

For 18-19 A GeV sequence, especially for the second centrality the ratio values for antikaons-kaons are equal, but also for antiprotons-protons, this repetitive plateau phenomenon showing a good correlation between the two ratio species (see Figures 17,19,20,23,24) [25,26,27].

We also calculated the dependence of the K-/K+ ratio to the  $\frac{\bar{p}}{p}$  ratio (see Figures 25-28). This shows some deviations, in the form of point returns of the ratio values, at certain energies. It is also found that the values in the graph are placed on "a vertical" for energy values between 10 A GeV and 14 A GeV, for the  $0 < y < 0.8$  rapidity interval and the range of collision parameters  $0 < b \leq 2.6$  Fm. A quasi-coincidence of values is observed for two successive energies of 18 A GeV and 19 A GeV, at  $0.5 < y < 1.4$  and  $2.6 < b \leq 5.2$  Fm, respectively. They may be areas of great interest in future experimental investigations. These predictions may indicate either a mixed phase transition, or a partial restoration of chiral symmetry, or even a first-order phase transition for the case of the  $0.5 < y < 1.4$  rapidity interval, for the range of energies 18-21 A GeV [27].

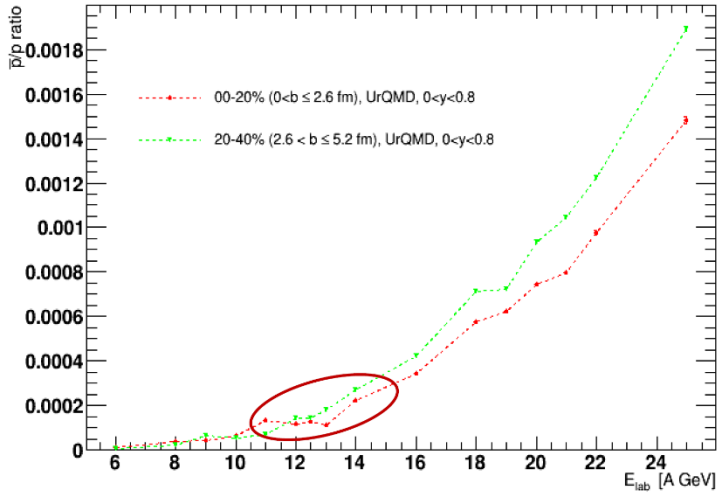


Fig 23.  $\frac{\bar{p}}{p}$  ratio distribution for two centralities,  $0 < y < 0.8$  rapidity interval and different collision energies, UrQMD [27]

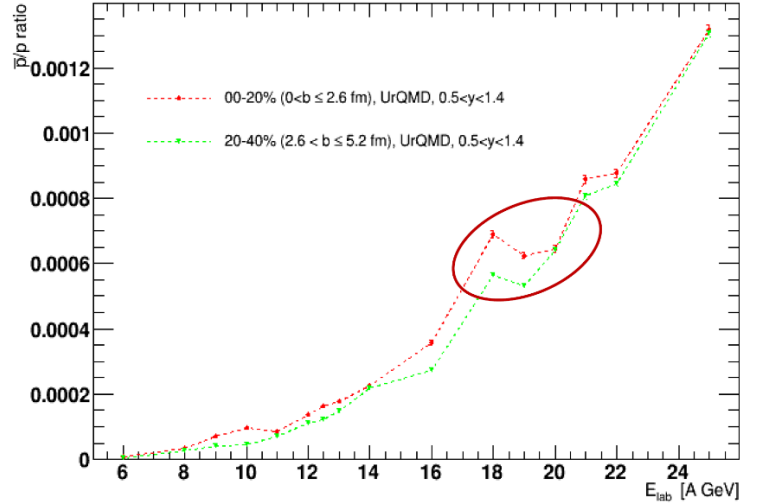


Fig 24.  $\frac{\bar{p}}{p}$  ratio distribution for two centralities,  $0.5 < y < 1.4$  rapidity interval and different collision energies, UrQMD [27]

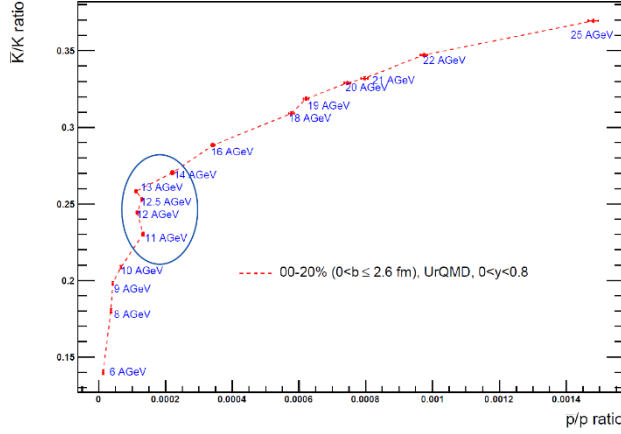


Fig 25.  $\frac{K^-}{K^+}$  to  $\frac{\bar{p}}{p}$  dependence for centrality 00-20% and rapidity interval:  $0 < y < 0.8$  [27]

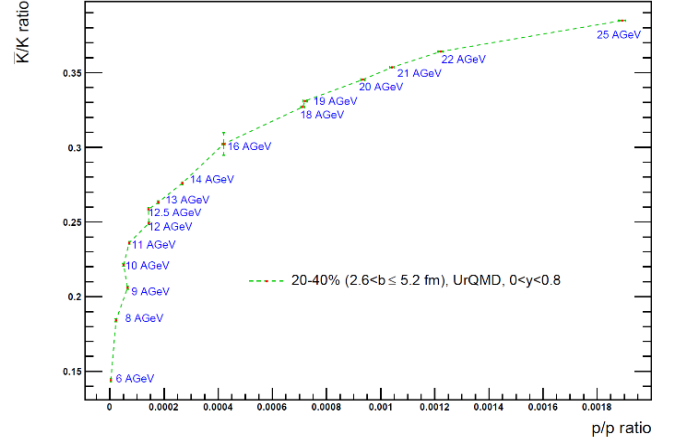


Fig 26.  $\frac{K^-}{K^+}$  to  $\frac{\bar{p}}{p}$  dependence for centrality 20-40% and rapidity interval:  $0 < y < 0.8$  [27]

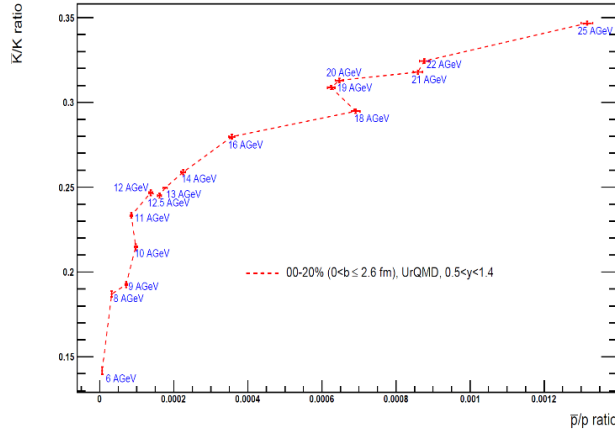


Fig 27.  $\frac{K^-}{K^+}$  to  $\frac{\bar{p}}{p}$  dependence for centrality 00-20% and rapidity interval:  $0.5 < y < 1.4$  [27]

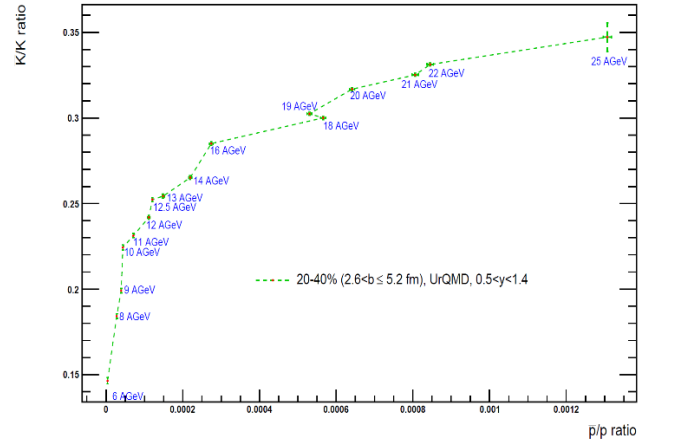


Fig 28.  $\frac{K^-}{K^+}$  to  $\frac{\bar{p}}{p}$  dependence for centrality 20-40% and rapidity interval:  $0.5 < y < 1.4$  [27]

## Conclusions

The main objective of the study is to search for signals of phase transitions in nuclear matter formed in Au-Au collisions, at the energies available at FAIR-GSI, using predictions from simulations. To achieve a phase transition in a nucleus-nucleus collision for an accelerator experiment, a medium with a temperature close to the transition value ( $T_c$ ) must be formed in the collision region. By analyzing the data based on simulations, I calculated transverse momenta and

used them to evaluate various physical quantities of interest, such as the temperature of the emission source. The temperature values calculated in this manner are in the vicinity of the critical temperature, considered to be in the range of 150-170 MeV. At such temperatures, we expect that the wide range of phenomena and processes that can occur in the overlapping region of colliding nuclei will be reflected in the QCD phase diagram. Such a diverse structure of events of interest may be connected to the first-order phase transition between hadronic and partonic matter.

Particle-antiparticle ratios are important for the study of exotic states and phase transitions in nuclear matter formed in relativistic heavy-ion collisions. They are useful in determining “freeze-out” parameters. Therefore, in the analysis of simulated data for Au-Au collisions in this study, the author used particle-antiparticle ratios. I presented results of numerical calculations for the energy range of 6-28 A GeV, in the laboratory system, for Au-Au collisions, for various centrality ranges, including ultra-central collisions. For easier comparison with certain measured or simulated data and experimental results, I also performed analyses for physically relevant quantities in the center-of-mass system.

In this thesis, I discuss the possibility of forming a mixed phase through a supposed pre-equilibrium phase transition, which I believe can be realized under conditions of a high baryonic potential for newly formed nuclear matter in heavy ion collisions. This transition, which may be pre-equilibrium, could be due to very intense interference between "strings" and could be realized under conditions of an extremely intense color magnetic field, when the gluonic channel becomes dominant. This transition will allow the creation of a sufficiently hot gluonic plasma, which will transform locally into a quark-gluon plasma, resulting in the appearance of a mixed phase, a phase which I consider to be produced in a somewhat "indirect" manner. In the case of such phenomena, we can talk about a partial restoration of chiral symmetry or a complete restoration of chiral symmetry. If the restoration is partial, a confined phase can still be preserved. But, of course, these remain subjects of theoretical debate and experimental confirmation. Estimates of the "microscopic Hubble constant" were made at chemical and, respectively, thermal "freeze-out". The thermal "freeze-out" temperatures were obtained from fits, using transverse momentum or transverse mass distributions for identified particles produced in the considered collisions, at different energies. The evolution time of the system until thermal "freeze-out" decreases with increasing energy. For the "microscopic Hubble constant" the following observations were made: at chemical "freeze-out" it increases with increasing energy, such that the rate of expansion of the



system is higher. It was noted that this constant is higher for chemical "freeze-out" than for kinetic "freeze-out". Therefore, the system reaches chemical "freeze-out" faster.

It was observed that near the critical point, fluctuations increase. Therefore, investigating fluctuations by analyzing ordinary and factorial moments of different orders, associated with the distributions of other physical quantities of interest, such as multiplicity, transverse momentum, and rapidity can be an efficient method of studying the region of the critical point localization. Higher moments of multiplicity distributions can be used to search for the critical point, for the QCD phase diagram in heavy ion collisions. For example, for the third-order moment, used in the definition of the asymmetry parameter ("skewness"), a change of sign is expected when the system's evolution trajectory in the phase diagram crosses the "border" (separation region) between phases. A similar result is expected in the case of the peak formation parameter ("kurtosis").

The results of the simulations for the antiparticle-particle ratios for central Au-Au collisions indicate an increase in the ratio with increasing incident energy, in agreement with other simulations and with experimental results at comparable or higher energies, for the same or similar types of collisions (Pb-Pb, U-Pb, Pb-Au).

I note that, beyond the influences of model hypotheses on the predictions of simulation codes, the results indicate significant changes in the quantities of interest with increasing energy. Moreover, in the two mentioned energy intervals, 10-14 A GeV and, respectively, 18-21 A GeV, for centrality classes  $0 < b \leq 2.6$  Fm and  $2.6 < b \leq 5.2$  Fm respectively, the formation of plateaus for the excitation function of antiparticle-particle ratios is observed, suggesting a possible mixed phase transition. The results of the analyses from simulations are compatible with other results based on different hypotheses, all indicating saturation/plateau behaviors, which can be correlated with the presence of phase transitions (mixed phase). These results must be validated by experimental data. The results I have obtained in this thesis, published in specialized journals, are compatible with the results obtained by other members of the CBM Experiment Collaboration.

## References

- [1]. Oana Ristea – Presentation notes, Relativistic Nuclear Physics (2020), Kolb EW, Turner MS. The Early Universe. Redwood City, CA: Addison-Wesley (1990), Coles P, Lucchin F. Cosmology. Chichester, UK: Wiley (1995), Mukhanov V. Physical Foundations of Cosmology. Cambridge, UK: Cambridge Univ. Press (2005), Denis Perret-Gallix, January 2013 - Journal of Physics Conference Series 454(1) DOI: 10.1088/1742-6596/454/1/012051, U. Heinz, arXiv:hep-ph/9902424v3 5 Mar 1999
- [2]. Jean Letessier, Johann Rafelski, - Hadrons and Quark–Gluon Plasma, Cambridge Press, 2002,
- [3]. Donoghue JF, et al. Dynamics of the Standard Model. Cambridge, UK: Cambridge Univ. Press (1992) A. Benvenuti et al. , Phys. Lett. B223, 490 (1989),
- [4]. S. Bethke , hep-ex/0211012
- [5]. B. Friman et al. (Editors), The CBM Physics Book, Lect.Notes Phys. Vol. 814 (Springer, 2011), Daniel Naegels - arXiv:2110.14504v1 [hep-th] 27 Oct 2021
- [6]. Al.Jipa - BRAHMS Collaboration Meeting, University of Copenhagen, “Niels Bohr” Institute, Denmark, 3-5 May 2006, Al.Jipa for the BRAHMS Collaboration – Annual Session of Scientific Communications of the Bucharest University - 26'th of May 2006 - invited talk, Al.Jipa for the Relativistic Nuclear Physics Group - National Physics Conference 13-18.IX.2005, București-Măgurele – oral talk
- [7]. Alam J-e, et al. Ann. Phys. 286:159 (2001); Alam J-e, et al. Ann. Phys.47:4171 (1993); Baier R, et al. Z. Phys.C 53:433 (1992); McLerran LD, Toimela T. Phys. Rev. D 31:545 (1985); Aurenche P, et al. Phys. Rev. D 58:085003 (1998), Aggarwal MM, et al. (WA98 Collab.) Phys. Rev. Lett. 85:3595 (2000), M.M. Aggarwa et al - arXiv:nucl-ex/0607018 v1 16 Jul 2006
- [8]. FAIR Baseline Technical Report 2006, <http://www.gsi.de/fair/reports/btr.html>
- [9]. J. F. Donoghue, E. Golowich and B. E. Holstein, Phys. Rev. D 34 (1986) 3434, H. Stoecker et al., Nucl. Phys. A 827 (2009) 624c.
- [10]. P. P. Bhaduri, A. K. Chauduri and S. Chattopadhyay - Phys. Rev. C 84 (2011) 054914
- [11]. M.Gazdzicki – Private conversation with the author, A Jipa - Private conversation with the author
- [12]. F. Becattini et al., Phys. Rev. Lett. 111, 082302 (2013), J. Stachel et al., J. Phys.: Conf. Ser. 509, 012019 (2014).
- [13]. S. Borsanyi et al., JHEP 09, 073 (2010). A. Bazavov et al., Phys. Rev. D 85, 054503 (2012)
- [14]. Y. Aoki et al., Nature 443, 675 (2006). C.S. Fischer, J. Luecker, C.A. Welzbacher, Phys. Rev. D 90, 034022 (2014)
- [15]. N. Tawfik, A.M. Diab, Phys. Rev. C 91, 015204 (2015). CERES Collaboration, B. Lenkeit et al. ,Nucl. Phys. A661, 23c (1999)
- [16]. Karsch F, Laermann E, Peikert A. Nucl. Phys. B 605:579 (2001), Ali Khan A, et al. (CP-PACS Collab.) Phys. Rev. D 63:034502 (2001), N.G. Tutas CBM Progress Report 2016, pages 193-194; M.Gazdzicki, M.Gorenstein - Acta Phys.Polon.B30(1999)2705
- [17]. T. Ablyazimov, et al. – European Physical Journal A53(3)(2017), T. Galatyuk et al. - Eur.Phys.J. A52(2016)131; K. Fukushima, Phys. Lett. B 695 (2011) 387; A. Andronic et al, Nuclear Phys. A 837 (2010) 65
- [18]. S. A. Bass et al., Prog. Part. Nucl. Phys. 41, 225-370 (1998); also available as nucl-th/9803035.; M. Bleicher, et al., J. Phys. G 25 (999) 11859 ; M. Belkacem et al. Phys. Rev. C58, 1727-1733 (1998); also available as nucl-th/9804058.

- [19]. Z.W. Lin et al, Phys. Rev. C72, 064901 (2005); Z.W. Lin et al, Phys. Rev. C64, 011902 (2001); B. Zhang et al, Phys. Rev.C61, 067901 (2000)
- [20]. S.Cioranu, Al.Jipa, M.Potlog – Romanian Reports în Physics 67(3)(2015)819-830
- [21]. STAR Colaborations (Thader) - Nucl.Phys.320 (2016)
- [22]. M Stefanov – Phys.Rev.Lett. B726(2013)691
- [23]. C.Ristea,...,N.G. Țuțuraș - Quark Matter 2014, Darmstadt, Germany
- [24]. Arsene et al., (BRAHMS Coll), Nucl. Phys. A 757, 1 (2005); B.B. Back et al., (PHOBOS Coll), Nucl. Phys. A 757, 28 (2005); J. Adams et al., (STAR Coll), Nucl. Phys. A 757, 102 (2005); K. Adcox et al., (PHENIX Coll), Nucl. Phys. A 757, 184 (2005)
- N. Xu and M. Kaneta, Nucl. Phys. A 698, 306 (2002); F. Becattini and G. Pettini, Phys. Rev. C 67,015205 (2003); W. Schmitz et al., J. Phys. G 28, 1861 (2002); J. Cleymans, H. Oeschler and K.Redlich, J. Phys. G 25, 281 (1999); J. Cleymans et al. Phys. Rev. C 57, 3319 (1998); F. Becattini, J. Cleymans, A. Keranen, E. Suhonen and K. Redlich, Phys. Rev. C 64, 024901 (2001)
- P. Braun-Munzinger, J. Stachel, J.P. Wessels, N. Xu, Phys. Lett. B 344, 43 (1995); P. Braun-Munzinger, J. Stachel, J.P. Wessels, N. Xu, Phys. Lett. B 365, 1 (1996); P. Braun-Munzinger, I. Heppe and J. Stachel, Phys. Lett. B 465, 15 (1999)
- C. Ristea, ... , N.G. Țuțuraș, ... - Romanian Reports in Physics, Vol.68, No.3, P.1060–1068, 2016
- [25]. Nicolae George Țuțuraș et al – CBM Progress Report 2018, page 173.
- [26]. Nicolae George Țuțuraș et al – CBM Progress Report 2020, pages 185-186.
- [27]. N. G. Țuțuraș et. al. – Romanian Reports in Physics 71(2019)303
- [28]. M.I. Gorenstein,M. Gazdzicki, K.A. Bugaev - Physics Letters B567(2003)175–178